Inorganic Chemistry

Article

pubs.acs.org/IC

Platinum(II) Complexes with O,S Bidentate Ligands: Biophysical Characterization, Antiproliferative Activity, and Crystallographic Evidence of Protein Binding

Carolin Mügge,[†,‡] Tiziano Marzo,[§] Lara Massai,[§] Jana Hildebrandt,[†] Giarita Ferraro,[∥] Pablo Rivera-Fuentes,[⊥] Nils Metzler-Nolte,[‡] Antonello Merlino,*[,∥,#] Luigi Messori,*[,§] and Wolfgang Weigand*[,†,⊗]

[†]Institute of Inorganic and Analytical Chemistry, Friedrich-Schiller-University Jena, Humboldtstraße 8, 07743 Jena, Germany

[‡]Inorganic Chemistry I - Bioinorganic Chemistry, Faculty of Chemistry and Biochemistry, Ruhr University Bochum, Universitaetsstrasse 150, 44801 Bochum, Germany

[§]Laboratory of Metals in Medicine, Department of Chemistry, University of Florence, Via della Lastruccia 3, 50019 Sesto Fiorentino, Firenze, Italy

[∥]Department of Chemical Sciences, University of Naples Federico II, via Cintia, Napoli I-80126, Italy

[⊥]Department of Chemistry, Chemistry Research Laboratory, University of Oxford, 12 Mansfield Road, Oxford OX1 3TA, United Kingdom

[#]CNR Institute of Biostructures and Bioimages, via Mezzocannone 16, Napoli I-80100, Italy

[⊗]Jena Center for Soft Matter (JCSM), Philosophenweg 7, 07743 Jena, Germany

Supporting Information

ABSTRACT: We recently characterized a series of novel platinum(II) compounds bearing a conserved O,S binding moiety as a bifunctional ligand and evaluated their solution behavior and antiproliferative properties in vitro against a representative cancer cell line. On the whole, those platinum compounds showed an appreciable stability in mixed dimethyl sulfoxide−aqueous buffers and promising in vitro cytotoxic effects; yet they manifested a rather limited solubility in aqueous media making them poorly suitable for further pharmaceutical development. To overcome this drawback, four new derivatives of this series were prepared and characterized based on a careful choice of substituents on the O,S bidentate ligand. The solubility and stability profile of these novel compounds in a reference buffer was determined, as well as the ligands' log $P_{o/w}$ value ($P_{o/w}$ = *n*-octanol−water partition coefficient) as an indirect measure for the complexes' lipophilicity. The antiproliferative properties were comparatively evaluated in a panel of three cancer cell lines. The protein binding properties of the four platinum compounds were assessed using the model protein hen egg white lysozyme (HEWL), and the molecular structures of two relevant HEWL-metallodrug adducts were solved. Overall, it is shown that a proper choice of the substituents leads to a higher solubility and enables a selective fine-tuning of the antiproliferative properties. The implications of these results are thoroughly discussed.

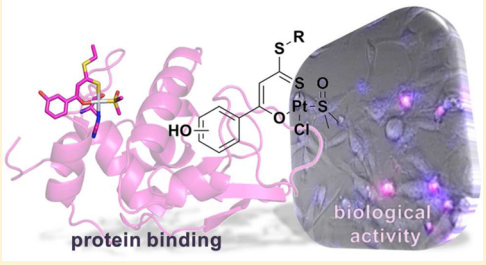

INTRODUCTION

Even though cisplatin is a well-established anticancer drug applied in many chemotherapy treatment schemes, still more platinum compounds are explored with a particular emphasis on their biomolecular interactions. In our endeavor to explore new possible anticancer drug candidates, we recently showed that a series of platinum(II) complexes bearing a bidentate O,S ligand based on *β*-hydroxy dithiocinnamic esters are of potential interest as experimental anticancer agents.[1] The biological properties of this class of platinum(II) compounds may be finely tuned through an appropriate choice of substituents both on the ring and on the alkyl chain R anchored to the O,S bidentate ligand (Chart 1). Yet, the compounds investigated so far manifested on the whole a rather limited solubility in aqueous buffers, which makes them poorly suitable for biological testing and for eventual clinical use.

The above arguments led us to perform a few specific chemical modifications on the reference scaffold to modulate and possibly improve the physicochemical properties while conserving the previously described favorable biological properties. The main strategy adopted here was to introduce a hydroxo group on the phenyl ring either in para or meta position while keeping the length of alkyl chains at the thioester subsite at a maximum of two carbon atoms. These structural modifications led to a set of four novel Pt(II) complexes that

Received: June 1, 2015
Published: August 17, 2015

DOI: 10.1021/acs.inorgchem.5b01238
Inorg. Chem. 2015, 54, 8560−8570

Chart 1. (O,S)Pt Complexes That Have Been Reported Previously (left)[1] and in This Work (right)

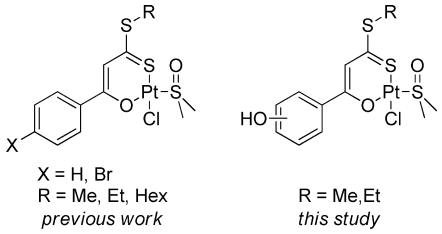

are represented in Chart 2. All discussed compounds share the same metal pharmacophore consisting of a platinum(II) center coordinated by the bidentate O,S ligand, by dimethyl sulfoxide (DMSO) through its S donor and by a chlorido ligand to give a square-planar constitution around the Pt(II) center. Compared to their parent compounds, the various complexes only differ in the nature of two substituents on the bidentate O,S ligand, yet these modifications are believed to have a considerable impact on bioavailability, reactivity, and biological activity of these platinum(II) compounds.

The aim of this study was to improve the aqueous solubility of these compounds, while retaining the favorable biological properties found earlier, and to understand the molecular interactions of these compounds with biomolecules in detail.

Toward this aim, the interaction of these compounds with a model protein, hen egg-white lysozyme (HEWL), was investigated in greater detail by applying electrospray ionization (ESI) mass spectrometric, UV−vis spectroscopic, and X-ray crystallographic techniques. Two crystal structures for the resulting Pt-HEWL adducts were solved.

Studies of this kind are of particular interest in metallodrug research, since in recent times, evidence has been gathered that metal−protein interactions may play an important role in the biological activity of such compounds.[2−6] Platinum−protein adducts may indeed participate in disfavorable processes, resulting in toxification, local accumulation, or even deactivation[7] of the pharmacophore. On the other hand, they may as well take part in selective transport- and uptake mechanisms;[8] even the role of proteins as "drug reservoir" is discussed.[9] Selective inactivation of enzymes involved in cancer generation and progression could also be exploited through the proper choice of substituents around the metal center. Even though the role of such processes for effective cancer therapy is not yet fully understood, it is of utmost importance to explore the molecular processes that lead to either selective or unselective binding of metallodrugs to proteins. This knowledge can then contribute to the greater picture that evolves from the manifold facets of the bioactivity of Pt-based metallodrugs.

HEWL, as was used as model protein here, is an ideal candidate for the complementary approach to investigate metal−protein adducts applied in this study: It is small (129 amino acids) and bears numerous positively charged amino acid side chains at the surface−making it well-suitable for ESI mass spectrometry (MS)-based investigations.[10−12] It is furthermore a well-recognized model protein for X-ray crystallographic investigations since it easily crystallizes and makes structural studies possible.[13,14]

EXPERIMENTAL SECTION

Syntheses. *General Remarks.* All syntheses were performed under inert conditions (Ar or N_2 atmosphere) using standard Schlenk techniques. Solvents were dried (dimethylformamide (DMF), tetrahydrofuran (THF), diethyl ether) or degassed (water) prior to their use in syntheses by established methods. Most starting materials were purchased from common suppliers. For column chromatography, silica gel of the type VWR Kieselgel 60 was used. Acetophenone derivatives **1** and **2** as well as the β-hydroxy dithiocinnamic methyl esters **3a**, **4a**, **5a**, and **6a** were prepared according to previously published methods.[15,16] Reference compounds **11** and **12** were prepared according to a procedure published earlier.[1] Analytical data of all other precursor compounds can be found in the Supporting Information.

Analyses. Elemental analyses of C, H, and S were performed on a LECO CHNS-931 instrument (Jena) or a Elementar Hanau vario EL device (Bochum). Obtaining proper elemental analyses proved to be difficult since the simultaneous presence of the elements Pt, S, and Si led to the formation of various undetectable or falsely detected combustion products. NMR spectra were recorded on a 200, 400, or 600 MHz instrument Bruker AVANCE 200, AVANCE 400, or Ultrashield+ AVANCE 600, respectively. Measurements took place at 200.13, 400.13, 600.13 MHz (^{1}H) or 50.33, 100.63, 150.94 MHz (^{13}C). The deuterated solvent served as an internal standard for ^{1}H and ^{13}C{^{1}H} NMR spectra. Signal assignment was confirmed by H,H COSY, HMBC, and HSQC experiments. For Pt(II) complexes **9**/**10**, some characteristic signals were obscured by solvent residual signals in ^{1}H or ^{13}C spectra. Therefore, data of **9b**/**10b** were recorded in acetone-d_6 and THF-d_8 to obtain complementary data with all signals. FT-IR spectra were measured on a Bruker Tensor27 device equipped with a MIRacle ATR unit. Mass spectra (FAB, ESI, DEI) were recorded on an instrument SSQ 710 (Finnigen MAT) and MAT95XL. Ionization was performed at 70 eV. UV−vis spectra were recorded in *n*-octanol using a 96-well plate format and a Tecan Saphire[2] plate reader.

*General Procedure: tert-Butyl dimethylsilyloxy β-hydroxy dithiocinnamic alkyl Esters **3/4**.* The *tert*-butyl dimethylsilyloxy (TBDMS)-protected acetophenone derivative **1** or **2** (5 g, 20 mmol) was dissolved in diethyl ether (50 mL) and transferred into a precooled suspension (−78 °C) of potassium-*tert*-butoxylate (KO^{t}Bu, 4.5 g, 40 mmol) in diethyl ether (50 mL). Carbon disulfide (CS_2, 1.7 mL, 28 mmol) was then slowly dropped into the solution. The mixture was stirred at −78 °C for 3 h and then allowed to warm to room temperature. After addition of the respective alkyl halide (20 mmol iodomethane or iodoethane), the mixture was stirred in darkness for further 15 h at room temperature. The suspension was then acidified with sulfuric acid (100 mL 2 M aqueous solution), and the evolving two-phased system separated. The aquatic phase was extracted with dichloromethane (3×), and the combined organic solutions were washed with water (3×), followed by drying with sodium sulfate. After filtration, the crude product was purified by column chromatography on silica gel (eluent: dichloromethane/hexane 1:1) and dried under vacuum.

*General Procedure: Hydroxy-Substituted β-Hydroxy dithiocinnamic alkyl Esters **5/6**.* The TBDMS-protected starting material **3**/**4** (2 mmol) was dissolved in THF (30 mL), and tetrabutyl ammonium fluoride (TBAF; 4 mL of 1 M solution in THF) was added. The suspension was stirred for 5 d, after which sulfuric acid (35 mL 2 M aqueous solution) was added, and the mixture stirred for another 3 h. The solution was extracted with dichloromethane (3×), washed with water (3×), and dried over sodium sulfate. The crude product was obtained after removal of the solvents and purified via column chromatography on silica gel with dichloromethane as eluent.

*General Procedure: Platinum(II) Complexes with O,S-Chelating β-Hydroxy dithiocinnamic Esters, Chloride, and Dimethyl Sulfoxide as Ligands **7−10**.* Sodium hydride (NaH, 17.5 mg 60% suspended in mineral oil, 0.438 mmol) was suspended in THF (5 mL) and transferred into a solution of the desired β-hydroxy dithiocinnamic ester **3−6** (0.438 mmol) in THF (15 mL). The solution was stirred at room temperature for 30 min and then slowly dropped into a suspension of potassium tetrachloroplatinate (K_2PtCl_4, 200 mg, 0.482 mmol in 2 mL of water), which was pretreated with DMSO (70 μL) until the precipitation of a white solid indicated the formation of

DOI: 10.1021/acs.inorgchem.5b01238
Inorg. Chem. 2015, 54, 8560−8570

DMSO−platinum species. The reaction mixture was stirred at room temperature until thin-layer chromatography control showed no starting material (typically 1−3 d). Workup included removal of the solvents in vacuo, uptake of the remainder in a proper solvent (typically dichloromethane or acetone), filtration of byproducts or liquid−liquid extraction, and column chromatography on silica gel, followed by precipitation from the eluent with pentane.

Chlorido-(1-(3′-hxdroxy)-3-(methylthio)-3-thioxo-prop-1-en-1-olate-O,S)-(dimethyl sulfoxide-S)-platinum(II) ***9a***. Dissolution in dichloromethane/acetone, column chromatoghaphy with dichloromethane/acetone 10:1. Yield 132 mg (51%) as orange powder. Anal. Calcd for $C_{12}H_{15}ClO_3PtS_3 \cdot 0.4$ pentane: C 29.88, H 3.55, S 17.09%; found C 30.29, H 3.18, S 16.40%. ^{1}H NMR (600 MHz, acetone-d_6) δ 8.82 (s, 1H, Ar−OH), 7.64−7.50 (m, 2H, Ar−H2, Ar−H6), 7.30 (m, 1H, Ar−H5), 7.22 (s, 1H, $CHCS_2$), 7.12−7.02 (m, 1H, Ar−H4), 3.68 (s w/Pt satellites, $^3J_{Pt-H}$ = 24.3 Hz, 6H, CH_3(DMSO)), 2.70 (s, 3H, SCH_3). ^{13}C NMR (151 MHz, acetone-d_6) δ 182.3 (CS_2), 175.3 (COPt), 159.0 (s, Ar−C3), 139.7 (Ar−C1), 131.0 (Ar−C5), 120.3 (Ar−C4), 120.0 (Ar−C6), 115.7 (Ar−C2), 111.8 ($CHCS_2$), 47.0 (2C, $^2J_{Pt-C}$ = 56.2 Hz, CH_3(DMSO)), 17.9 (SCH_3). IR (ATR) $\tilde{\nu}$ = 3302, 3024, 3007, 2954, 2921, 2853, 1734, 1662, 1611, 1583, 1511, 1491, 1472, 1445, 1426, 1402, 1366, 1329, 1291, 1248, 1210, 1092, 1069, 1029, 997, 973, 962, 933, 910, 865, 796, 778 cm^{-1}. MS (FAB in nba) m/z = 534 $[M]^+$, 498 $[M\text{-}Cl]^+$. UV [*n*-octanol; λ_{max}, nm (ε ± sd, M^{-1} cm^{-1})]: 349 (13 800 ± 500), 429 (10 000 ± 750).

Chlorido-(1-(3′-hxdroxy)-3-(ethylthio)-3-thioxo-prop-1-en-1-olate-O,S)-(dimethyl sulfoxide-S)-platinum(II) ***9b***. Dissolution in dichloromethane/acetone, column chromatoghaphy with dichloromethane/acetone 10:1. Yield 132 mg (55%) as orange powder. Anal. Calcd for $C_{13}H_{17}ClO_3PtS_3 \cdot 0.15$ pentane: C 29.55; H 3.39; S 17.21%; found C 29.48, H 3.37, S 17.20%. ^{1}H NMR (200 MHz, THF-d_8) δ 8.72 (s, 1H, Ar−OH), 7.59−7.33 (m, 2H, Ar−H2, Ar−H6), 7.33−7.03 (m, 2H, Ar−H5, $CHCS_2$), 7.03−6.79 (m, 1H, Ar−H4), 3.60 (s w/Pt satellites, $^3J_{Pt-H}$ = 23.7 Hz, 6H, CH_3(DMSO), overlaid by THF), 3.25 (q, $^3J_{H-H}$ = 7.4 Hz, 2H, SCH_2), 1.42 (t, $^3J_{H-H}$ = 7.4 Hz, 3H, SCH_2CH_3). ^{1}H NMR (250 MHz, acetone-d_6) δ 8.80 (s, 1H, Ar−OH), 7.59−7.46 (m, 2H, Ar−H2, Ar−H6), 7.31 (t, $^3J_{H-H}$ = 8.1 Hz, 1H, Ar−H5), 7.21 (s, 1H, $CHCS_2$), 7.16−7.01 (m, 1H, Ar−H4), 3.68 (s, w/Pt satellites $^3J_{Pt-H}$ = 24.1 Hz, 6H, CH_3(DMSO)), 3.29 (q, $^3J_{H-H}$ = 7.4 Hz, 2H, SCH_2), 1.44 (t, $^3J_{H-H}$ = 7.4 Hz, 3H, SCH_2CH_3). ^{13}C NMR (50 MHz, THF-d_8) δ 180.7 (CS_2), 175.6 (COPt), 159.4 (Ar−C3), 139.8 (Ar−C1), 130.5 (Ar−C5), 120.3 (Ar−C6), 119.51(Ar−C4), 115.7 (Ar−C2), 112.1 (s), 111.3 ($CHCS_2$), 46.7 (2C, CH_3(DMSO)), 29.3 (SCH_2), 13.9 (SCH_2CH_3). ^{13}C NMR (63 MHz, acetone-d_6) δ 181.15 (CS_2), 175.46 (COPt), 158.86 (Ar−C3), 139.58 (Ar−C1), 130.83 (Ar−C5), 120.26 (Ar−C6), 119.86 (Ar−C4), 115.55 (Ar−C2), 111.93 ($CHCS_2$), 46.85 (2C, CH_3(DMSO)), 13.63 (SCH_2CH_3). Signal of SCH_2 overlaid by solvent signal. IR (ATR) $\tilde{\nu}$ = 3335, 3005, 2981, 2921, 2853, 1662, 1609, 1581, 1507, 1490, 1466, 1441, 1429, 1402, 1311, 1288, 1255, 1237, 1198, 1138, 1098, 1069, 1028, 997, 972, 931, 9110, 884, 796, 779 cm^{-1}. MS (ESI) m/z = 571 $[M + Na]^+$, 512 $[M\text{−}Cl\text{-}H]^+$. UV [*n*-octanol; λ_{max}, nm (ε ± sd, M^{-1} cm^{-1})]: 352 (19 900 ± 3000), 429 (12 000 ± 850).

Chlorido-(1-(4′-hxdroxy)-3-(methylthio)-3-thioxo-prop-1-en-1-olate-O,S)-(dimethyl sulfoxide-S)-platinum(II) ***10a***. Dissolution in dichloromethane/acetone, column chromatography with dichloromethane/acetone 10:1. Yield 136 mg (58%) as orange powder. Anal. Calcd for $C_{12}H_{15}ClO_3PtS_3 \cdot 0.35$ pentane: C 29.53; H 3.46; S 17.20%; found C 29.56, H 3.33, S 16.49%. ^{1}H NMR (200 MHz, acetone-d_6) δ 9.28 (s, 1H, Ar−OH), 8.03 (d, $^3J_{H-H}$ = 8.9 Hz, 2H, Ar−H2, Ar−H6), 7.23 (s, 1H, $CHCS_2$), 6.92 (d, $^3J_{H-H}$ = 8.8 Hz, 2H, Ar−H3, Ar−H5), 3.66 (s w/Pt satellites, $^3J_{Pt-H}$ = 24.3 Hz, 6H, CH_3(DMSO)), 2.68 (s, 3H, SCH_3). ^{13}C NMR (50 MHz, acetone-d_6) δ 179.64 (CS_2), 175.0 (COPt), 162.4 (Ar−C4), 131.4 (2C, Ar−C2, Ar−C6), 129.3 (Ar−C1), 116.5 (2C, Ar−C3, Ar−C5), 110.8 ($CHCS_2$), 46.8 (2C, CH_3(DMSO)), 17.6 (SCH_3). ^{195}Pt NMR (128 MHz, DMSO-d_6) δ −3082 ppm. IR (ATR) $\tilde{\nu}$ = 3320, 2999, 2912, 2854, 1734, 1602, 1585, 1520, 1490, 1454, 1416, 1358, 1313, 1281, 1265, 1212, 1169, 1122, 1026, 980, 952, 934, 925, 842, 794 cm^{-1}. MS (FAB in nba) m/z = 534 $[M]^+$, 498 $[M\text{−}Cl^-]^+$. UV [*n*-octanol; λ_{max}, nm (ε ± sd, M^{-1} cm^{-1})]: 350 (17 000 ± 1050), 429 (15 100 ± 1500).

Chlorido-(1-(4′-hxdroxy)-3-(ethylthio)-3-thioxo-prop-1-en-1-olate-O,S)-(dimethyl sulfoxide-S)-platinum(II) ***10b***. Dissolution in dichloromethane/acetone, column chromatography with dichloromethane/acetone 10:1. Yield 175 mg (73%) as orange powder. ^{1}H NMR (400 MHz, THF-d_8) δ 9.10 (s, 1H, Ar−OH), 7.96 (d, $^3J_{H-H}$ = 8.8 Hz, 2H, Ar−H2, Ar−H6), 7.15 (s, 1H, $CHCS_2$), 6.78 (d, $^3J_{H-H}$ = 8.8 Hz, 2H, Ar−H3, Ar−H5), 3.59 (s w/Pt satellites, 6H, CH_3(DMSO) overlaid by THF), 3.24 (q, $^3J_{H-H}$ = 7.4 Hz, 2H, SCH_2), 1.40 (t, $^3J_{H-H}$ = 7.4 Hz, 3H, SCH_2CH_3). ^{1}H NMR (200 MHz, acetone-d_6) δ 9.29 (s, 1H, Ar−OH), 8.02 (d, $^3J_{H-H}$ = 8.9 Hz, 2H, Ar−H2, Ar−H6), 7.23 (s, 1H, $CHCS_2$), 6.93 (d, $^3J_{H-H}$ = 8.9 Hz, 2H, Ar−H3, Ar−H5), 3.66 (s w/Pt satellites, $^3J_{Pt-H}$ = 24.2 Hz, 6H, CH_3(DMSO)), 3.28 (q, $^3J_{H-H}$ = 7.4 Hz, 2H, SCH_2), 1.41 (t, $^3J_{H-H}$ = 7.4 Hz, 3H, SCH_2CH_3). ^{13}C NMR (101 MHz, THF-d_8) δ 178.03 (CS_2), 175.37 (COPt), 162.84 (Ar−C4), 131.36 (2C, Ar−C2, Ar−C6), 129.32 (Ar−C1), 116.39 (2C, Ar−C3, Ar−C5), 111.23 ($CHCS_2$), 46.70 (2C, CH_3(DMSO)), 29.05 (SCH_2), 13.97 (SCH_2CH_3). ^{13}C NMR (63 MHz, acetone-d_6) δ 175.41 (COPt), 162.46 (Ar−C4), 131.45 (2C, Ar−C2, Ar−C6), 129.33 (Ar−C1), 116.54 (2C, Ar−C3, Ar−C5), 111.19 ($CHCS_2$), 46.87 (2C, CH_3(DMSO)), 13.78 (SCH_2CH_3). Signal of SCH_2 overlaid by solvent signal; quaternary CS_2 not observed. IR (ATR) $\tilde{\nu}$ = 3326, 2999, 2963, 2924, 2865, 1726, 1602, 1522, 1490, 1460, 1449, 1417, 1360, 1346, 1308, 1281, 1260, 1170, 1121, 1025, 971, 850, 842, 793 cm^{-1}. MS (ESI) m/z = 570 $[M + Na]^+$, 512 $[M\text{−}Cl\text{-}H]^+$, 235. UV [*n*-octanol; λ_{max}, nm (ε ± sd, M^{-1} cm^{-1})]: 353 (17 200 ± 1050), 430 (14 200 ± 1800).

Spectrophotometric Experiments. UV−vis absorption spectra were recorded on a Varian Cary 50 UV−vis spectrophotometer in the range of 200−800 nm. Stock solutions (10 mM) of each compound were prepared by dissolving the complex under investigation in DMSO.

Solvolytic Stability. For solubility studies, UV−vis measurements were performed by diluting the compounds' stock solutions to 100 μM in tetramethylammonium acetate buffer (TMAA, 25 mM, adjusted to pH 7.4 with NaOH) with varying content of DMSO (final percentages 1%, 25%, 50% v/v). Spectra were collected for 24 h at room temperature (r.t.), operating in 10 min intervals during the first hour and in 1 h intervals afterward.

Reactivity toward Lysozyme. UV−vis measurements with HEWL were performed by diluting the compounds' stock solutions to 30 μM in TMAA. After the initial spectrum was recorded without protein, HEWL was added at 10 μM to yield a final metal/protein ratio of 3:1. Spectra were recorded over 72 h at r.t., operating in 10 min intervals during the first hour, in 1 h intervals to 24 h and finally in 3 h intervals to 72 h.

Computational Calculations. All calculations were performed using ORCA, version 2.8. Molecular orbitals were plotted using VMD. The optimized geometry of compound **9a** was obtained at the BP86/def2-TZVP(-f). The zeroth-order regular approximation (ZORA) was applied to correct for relativistic effects (Pt). Solvation effects were modeled using COSMO (water) as implemented in ORCA. The minimum found in the optimization step was characterized by harmonic vibrational analysis (all frequencies are positive). Vertical excitations were computed at the B3LYP/def2-TZVP(-f) level of theory using ZORA and COSMO (water) as described above.

Determination of Partition Coefficient − log $P_{o/w}$ by Shake Flask Method. For determination of log $P_{o/w}$ ($P_{o/w}$ = *n*-octanol/water partition coefficient) values by the shake-flask method, Millipore water and *n*-octanol were presaturated for a minimum time of 48 h, and the phases were allowed to separate for at least 24 h. Stock solutions of the respective compounds were prepared at 500 μM in presaturated *n*-octanol and diluted to a final concentration of 50 μM in the same solvent. Three mixtures for each compound were then prepared in micro reaction tubes with *n*-octanol/water ratios of 2:1, 1:1, and 1:2 (v/v) at a final volume of 1200 μL. The mixtures were vigorously shaken on a laboratory shaker for 60 min, centrifugated (10 min at 10 000 rpm) to separate the phases, and triplicate 100 μL aliquots of

DOI: 10.1021/acs.inorgchem.5b01238
Inorg. Chem. 2015, 54, 8560−8570

each phase were transferred onto a 96-well plate. UV−visible spectra were recorded between 230 and 600 nm on a Tecan Saphire^2 plate reader. Triplicate aliquot spectral data was averaged and baseline corrected, and $P_{o/w}$ values were calculated from the three individual volume ratio experiments, using the average absorbance data from 300 to 500 nm. The overall log $P_{o/w}$ value was then calculated from the average of three individual $P_{o/w}$ values.

Biological Assays. *Cell Culture and Passaging.* Cells were generally handled under sterile conditions in a laminar airflow cabinet. Cells were grown in high glucose Dulbecco's Modified Eagle's Medium (DMEM, Gibco), supplemented with 1% sodium pyruvate, 1% L-glutamine, 100 units·mL^{-1} PenStrep, and 10% fetal bovine serum (FCS, Biochrom) and containing phenol red. For microscopy applications, equally supplemented DMEM without phenol red was used. The cells were maintained in 10 cm cell culture dishes at 37 °C in a humidified incubator under an atmosphere containing 10% CO_2. Dividing of cells was usually performed at 90% cell confluence by standard procedures and until the 50th passage at most.

For assays, the adherent cells were harvested using trypsin−EDTA (Gibco), and the reaction was stopped by addition of fresh DMEM/10% FCS. Cells were counted using a Bio-Rad automated cell counter and 10 000 cells/well seeded onto 96-well plates in a final volume of 100 μL of DMEM/10% FCS. Blank wells were filled with medium without cells. The plates were incubated for 1 d prior to drug addition to allow for cells to attach. For fluorescence microscopy, HeLa and MCF7 cells were seeded onto 8-well microscopy slides (IBIDI) at 25 000 cells/well in 250 μL DMEM/10% FCS without phenol red and incubated for 1 d prior to drug addition.

Drug Addition and Viability Assays. Stock solutions of investigational samples were prepared at 50 mM in DMSO, stock solutions of cisplatin were prepared in phosphate-buffered saline (PBS). For each independent experiment, fresh stock solutions were prepared from powder. All samples were diluted to the desired concentration in DMEM/10% FCS immediately prior to their addition to cells in a range between 500 and 1 μM. In separate control experiments, the effect of DMSO present in the different sample concentrations was tested. No significant effect on cell growth at drug concentrations close to respective IC_{50} values was witnessed.

For drug addition to the cells, medium was removed from the wells, and 90 μL of fresh drug-containing medium or pure medium (for controls and blanks) was added to the wells, using four wells for each concentration. After an incubation time of 70 h at 37 °C, 10 μL of PrestoBlue cell viability agent (Life Technologies) was added, and the cells further incubated to 72 h. Fluorescence intensities were read on a Tecan Saphire^2 plate reader with λ_{Ex} = 560 nm and λ_{Em} = 590 nm.

Data Handling. IC_{50} values were calculated from the inflection point of the sigmoidal curve fit, using the original, uncorrected data. The regression was based on formula 1:

$$y = A2 + \frac{A1 - A2}{1 + \left(\frac{x}{x_0}\right)^p} \quad (1)$$

with A1 and A2 being the lower and upper asymptote, respectively, p being the power/slope, and x_o resembling the inflection point and thus the IC_{50} value in micromolar.

Fluorescence Microscopy. Sample solutions of **9b** were prepared from DMSO stock solutions as stated above, using DMEM/10%FCS without phenol red. Medium from preincubated microscopy slides was replaced by 250 μL of drug-containing medium at concentrations above the determined IC_{50} (50 μM), ca. IC_{50} (20 μM for HeLa and 30 μM for MCF7), and below IC_{50} (10 μM). Slides were incubated for 72 h to achieve the desired cellular reactions.

4′,6-Diamidin-2-phenylindol (DAPI) and propidium iodide (PI) were stored as separate stock solutions in PBS. Immediately prior to the experiment, a 10× concentrated DAPI/PI staining solution was prepared and added to the incubated cells to give final concentrations of 50 μg/mL DAPI and 20 μg/mL PI. No substitution of medium or washing was performed to retain all, living and dead, cells. Stained cells were reincubated for 1 h before microscopy.

Fluorescence micrographs were collected on a Olympus IX-81 fluorescence microscope, equipped with a XM10 monochrome CCD camera and controlled by Cell^M software. Filter cubes with λ_{Ex} = 330−385 nm, λ_{Em} = 420+ nm (for DAPI-stained cells) and with λ_{Ex} = 530−550 nm, λ_{Em} = 590+ nm (for PI-stained cells) were used to record the micrographs at 200-fold magnification.

Hen Egg-White Lysozyme Interaction Studies—Electrospray Ionization Mass Spectrometry. The stock solution of HEWL (Sigma L7651) was prepared in Millipore water at 1 mM and stored at −20 °C until usage. DMSO stock solutions (10 mM) of the investigational complexes were prepared and introduced into TMAA (25 mM, pH 7.4) at 300 μM containing 100 μM protein, to give a final metal/protein molecular ratio of 3:1. Samples were incubated at 37 °C for 24 or 72 h.

Electrospray ionization mass spectra of the metal−protein mixtures were recorded from samples generated through 20-fold dilution with water in an LTQ-Orbitrap high-resolution mass spectrometer (Thermo, San Jose, CA, USA), equipped with a conventional ESI source (direct introduction, flow rate 5 μL/min). The following standardized working conditions were applied: spray voltage 3.1 kV, tube lens voltage 230 V, capillary voltage 45 V, and capillary temperature 220 °C. Sheath and auxiliary gases were set at 17 au and 1 au, respectively. Data was acquired with a nominal resolution of 100 000 (at m/z 400), using Xcalibur 2.0 software (Thermo); monoisotopic and average deconvoluted masses were obtained with the integrated Xtract tool.

Hen Egg-White Lysozyme Interaction Studies−Crystallographic Data. *Crystallization of the Adducts with Hen Egg-White Lysozyme.* Hen egg-white lysozyme was crystallized by vapor diffusion method, using the hanging drop technique. Lysozyme, dissolved in purified water and concentrated at 30 mg/mL, was mixed with an equal volume of 20% ethylene glycol, 0.1 M sodium acetate (pH 4.5), and 0.6 M sodium nitrate. Crystals grew in 1−3 d. These crystals were soaked in solutions containing **9a** or **9b**, dissolved in DMSO, and added to the mother liquor of each crystal. Final concentration was 15% ethylene glycol, 0.075 M sodium acetate (pH 4.5), 25% DMSO, 0.4 M sodium nitrate (pH 4.5). UV−visible screening of the compounds suggested that the (O,S) ligand is retained under these conditions (data not shown). This procedure has been already used to obtain crystals of adduct between lysozyme and other metallodrugs.[17,18]

Data Collection, Structure Solution, and Refinement. X-ray diffraction data from soaked crystals were collected at the CNR Institute of Biostructures and Bioimages in Naples using a Cu rotating anode. In all cases, diffraction patterns were recorded at 100 K using a CCD detector with an oscillation range of 1.0 degree per frame, an exposure time of 5.0−8.0 seconds per frame, and a crystal-to-detector distance of 45 mm. To avoid possible structural heterogeneities due to a short soak in the cryoprotectant solution, data sets were obtained after freezing the crystals without a cryoprotectant solution, as previously done in other works.[18,19] Diffraction images were processed with the HKL2000 program suite.[20] Statistics of the data collections of best HEWL-**9a** and HEWL-**9b** crystals are summarized in Table S1.

The structure of lysozyme from PDB code 4J1A[21] without water molecules and ligands was used as a starting model for crystallographic refinements. Refinement was performed using the program REFMAC[22] of the CCP4 suite.[23] Platinum (and thus ligand atoms) occupancies were manually adjusted, until no peaks were observed on the Pt center in the difference Fourier ($F_o - F_c$) electron density maps. Model building and electron density map fitting were performed using WinCoot.[24] Refinements suggest occupancy values close to 0.6 with B-factor values that fall within 22−31 Å^2 for Pt atoms. Statistics of the refined structures are summarized in Table S2. The structures were deposited in the Protein Data Bank under the accession codes 4Z41 and 4Z3M for HEWL-**9a** and HEWL-**9b**, respectively.

RESULTS

Synthesis and Characterization of the Novel Platinum(II) Compounds. The compounds were prepared

DOI: 10.1021/acs.inorgchem.5b01238
Inorg. Chem. 2015, 54, 8560−8570

Scheme 1. Synthetic Procedure toward the Pt(II) Complexes[a]

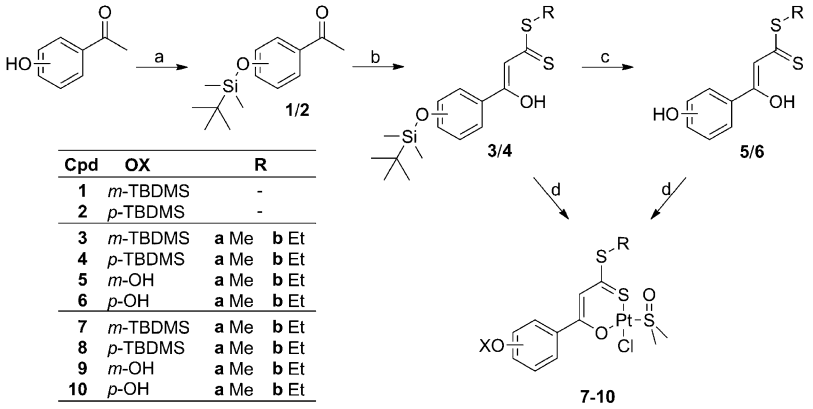

Cpd	OX	R	
1	*m*-TBDMS	-	
2	*p*-TBDMS	-	
3	*m*-TBDMS	**a** Me	**b** Et
4	*p*-TBDMS	**a** Me	**b** Et
5	*m*-OH	**a** Me	**b** Et
6	*p*-OH	**a** Me	**b** Et
7	*m*-TBDMS	**a** Me	**b** Et
8	*p*-TBDMS	**a** Me	**b** Et
9	*m*-OH	**a** Me	**b** Et
10	*p*-OH	**a** Me	**b** Et

7-10

[a](a) TBDMS-Cl, imidazole, DMF, r.t.; (b) [i] 2 equiv of KO^{t}Bu, CS_2, [ii] Hal-R, [iii] H^+/H_2O, diethyl ether, −70 °C → r.t.; (c) NBu_4F, H^+, THF, r.t.; (d) [i] NaH, [ii] aqueous K_2PtCl_4/2 equiv of DMSO, THF, r.t.

following procedures reported earlier (Scheme 1).[1,15,16] The main steps of the ligand synthesis involved the preparation of TBDMS-protected acetophenone derivatives **1**/**2** and subsequent conversion with carbon disulfide and with the respective alkyl halide. The so-prepared *β*-hydroxy dithiocinnamic acid esters **3**/**4** still contained the TBDMS group, which was cleaved using TBAF to yield **5**/**6**, containing a hydroxo group either in meta (**5**) or para (**6**) position. Platinum(II) complexes **7**−**10** were then prepared from potassium tetrachloroplatinate(II) (K_2PtCl_4) and ligands **3**−**5** in the presence of a base and DMSO. Under the reaction conditions applied for this synthesis, the TBDMS group of **3**/**4** was retained, and complexes **7**/**8** were isolated in moderate yields (30−60%). Ligands **5**/**6** were also successfully coordinated to the Pt(II) center; complexes **9**/**10** were obtained in yields of 50−70%. To explore potential optimized pathways toward **9** and **10**, cleavage of the protecting group was also attempted from complexes **7**/**8**, using the same procedure that was successfully applied for the ligands. In these cases decomposition of the complexes was observed, so that the synthesis of **9**/**10** was only performed via the first described pathway. All synthesized compounds were characterized by NMR and IR spectroscopic methods, MS, and elemental analysis.

In NMR spectra of compounds **1**, **2**, **3**, **4**, **7**, and **8**, the presence of the TBDMS group was clearly established by two singlets at ca. 1 and 0.2 ppm (in ^{1}H) and signals at ca. 18 and −4 ppm (in ^{13}C), belonging to the *α* and *β* methyl groups relative to Si, respectively.

Subsequent deprotection led to a loss of the TBDMS signals. When $CDCl_3$ was used as solvent, the formed phenyl−OH group gave no signal in ^{1}H NMR spectra. In acetone-d_6 or THF-d_8, the phenyl−OH signal could be observed at ca. 8−9 ppm.

Characteristic NMR signals belonging to the ligands' structural features are comparable to those reported earlier.[1,15,16] The most representative signals are those of the methine group at 6.8 and 107−108 ppm in the ^{1}H and ^{13}C NMR spectra, respectively, and to the *β*-hydroxy group, which appears as a sharp singlet at ca. 15.0−15.3 ppm in the ^{1}H NMR spectra. Further signals include those belonging to the sulfur-bound CH_2 and CH_3 groups, which appear at ca. 3.25 and 2.65 ppm for the S-Me and S-Et sites, respectively, in the ^{1}H NMR spectra and at 28−29 and 17.7 ppm, respectively, in the ^{13}C NMR spectra. The position of the substituents at the aromatic moiety can clearly be established from the coupling pattern in the aromatic region of the ^{1}H NMR spectra (6.5−8 ppm): two apparent doublets, indicative of the AA′BB′ spin system, are observed for compounds with a para-substituent, and several multiplets are observed for those with meta substitution pattern.

Binding of the ligands toward platinum leads to few characteristic changes in the NMR spectra. Basically only the loss of the *β*−OH high-frequency signal and a shift of the signal belonging to the methine proton by ca. +0.4 to 7.0−7.2 ppm as well as a shift of the ^{13}C NMR signal of the methine carbon to 111−112 ppm indicate coordination toward Pt(II). The carbon atom of the CS_2 unit gives a ^{13}C NMR signal at 215−217 ppm in the free ligands and is massively shifted to lower frequencies of 180−182 ppm when coordinated to the Pt(II) core.

Pt(II)-coordinated DMSO constantly appears at 3.6−3.7 ppm with $^3J_{Pt-H}$ = 23.4−24.3 Hz in the ^{1}H NMR spectra and at 47 ppm in the ^{13}C NMR spectra, irrespective of the solvent, indicating no noteworthy influence of the substitution pattern on the binding properties of the DMSO ligand toward the metal center. This observation underlines the previously stated hypothesis that variations at the chelating unit do not significantly influence the nature of the presumed active center of the molecule and therefore make adaptions of the ligand possible that should eventually lead to optimized pharmacological features.

Obtaining mass spectra of whole complex molecular ions proved to be difficult; in many cases only the fragment after loss of the chloride ion could be recorded. In few cases, FAB ionization enabled the detection of the whole molecular ions.

Since the main goal of this study was to improve the solvolytic profile of the compounds, the four compounds with free hydroxyl groups at the aromatic moiety **9**/**10** were chosen to be investigated in detail for this study (Chart 2). Compounds **11** and **12** from earlier studies were considered as a reference.

Behavior in Solution. Solubility in aqueous media is a critical factor for the pharmaceutical use of these compounds. Thus, we analyzed the influence that the above-mentioned substituents produce on water solubility. Solubility of complexes **9**/**10** was qualitatively assessed through spectrophotometric analysis. Also, quantification in terms of their ligands' water/octanol partition coefficient was performed.

DOI: 10.1021/acs.inorgchem.5b01238
Inorg. Chem. 2015, 54, 8560−8570

Chart 2. Compounds That Were Investigated in More Detail for This Study

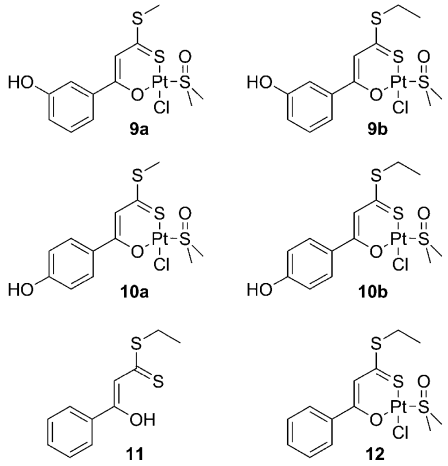

Stability in Solution through Spectrophotometric Analysis. The behavior of these four platinum(II) complexes in solution was analyzed through continuous monitoring of their visible bands over 24 h after dissolution in DMSO−TMAA (TMAA 25 mM) buffer mixtures. The compounds share a common chromophore expressed as major absorption bands, centered at ∼350−360 nm and at 410−420 nm. The exact position and shape of the spectrum differs with the varying substituent positions. The visible bands of compound **9a** were assigned based on time-dependent density functional theory (TD-DFT) calculations (see the Experimental Section for details). These calculations show that the absorptions around 415 and 350 nm arise from ligand-to-metal charge-transfer interactions (Figures S1 and S2) and are therefore suitable to probe metal dissociation.

Time-dependent spectral profiles are shown in Figure 1 and Figures S3−S5. Some small spectral changes are observed with time. It is straightforward to assign these spectral modifications to progressive aquation of the chlorido group, followed by some degree of precipitation.

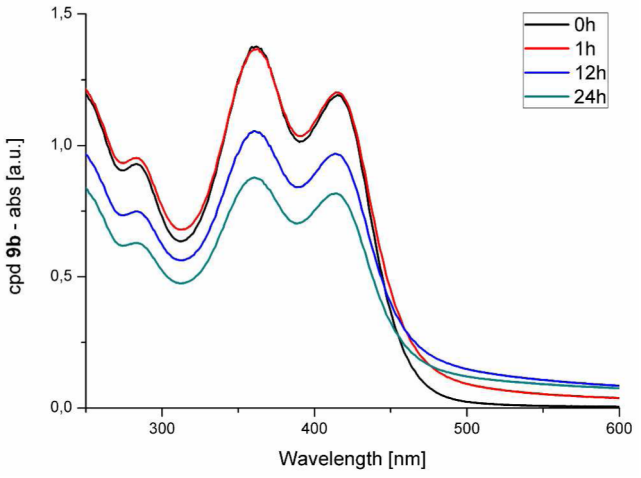

Figure 1. Time course UV−vis spectra of platinum compound **9b** dissolved in 25% DMSO−75% 25 mM TMAA (pH = 7.4), over 24 h at room temperature. Concentration of the complex is 100 μM. Spectra were recorded at t = 0 h (black line), 1 h (red line), 12 h (blue line), and 24 h (green line).

It is unlikely that DMSO is released under these experimental conditions as the DMSO concentration in solution is very high. Also, we found evidence of an aquation reaction taking place through exchange of the chlorido ligand in earlier studies.[1]

Time-dependent spectral profiles show characteristic isosbestic points that are suggestive of the occurrence of an equilibrium between two species: the chlorido complex and the corresponding aqua species. Apparently the aquation process is relatively slow with a half-life of ∼5−8 h.

Some peculiar reactivity of compounds **9**/**10** was found in dependence of the used amount of DMSO (Figure S3−S5): at 25 vol % DMSO, no significant shifts of the band maxima are evident (Figure S4). When the amount of DMSO is increased to 50 vol %, a hypsochromic shift of ∼10 nm can be seen for both complex bands (Figure S5). This might indicate an enforced substitution of chloride by DMSO or simply the formation of a solvation sphere of DMSO around the Pt(II) center.

The electronic structure of the O,S chelating unit and the adjoining moieties are strongly influenced by the nature of the monodentate ligands trans to S and O. According to our TD-DFT results, both major bands observed in the compounds' UV−vis spectra involve interactions of the (O,S) ligand chromophore and the metal. On the contrary, experimental results show that the free ligand gives a completely different spectral profile—some representative spectra can be found in Figure S6. A loss of the bidentate donor molecule can thus be ruled out in all of our investigations.

Solubility in Aqueous Medium—Determination of log $P_{o/w}$ Values. The solubility of organic compounds is frequently quantified by their log $P_{o/w}$ value, that is, measures of the water/*n*-octanol partition coefficient, determined through the shake-flask method.[25,26] In recent times, this quantification method has also been introduced in medicinal inorganic research scopes for determining the polarity of metal compounds.[27−30] It appears indeed to be a straightforward idea since the method is simple and versatile at the same time (basically, a defined stock solution of the compound in water or *n*-octanol is mixed with the respective counter-solvent followed by determination of its concentration in both phases by any appropriate method). However, this method will not give reliable results when using metal complexes that are prone to hydrolysis reactions in aqueous medium. As an alternative method to determine the polarity of the compounds discussed here, the well-established HPLC method[31−33] was tested; however, the compounds under investigation underwent hydrolysis quickly at conditions appropriate for this approach.

It is indeed not useful to determine the polarity of the complexes in a water/*n*-octanol mixture. If the experiment is planned in a time frame shorter than needed for full hydrolysis, the system will not be in equilibrium state due to ongoing aquation reactions (even if slowed by the addition of appropriate salts). If the experiment is performed at true equilibrium state, as required for a correct determination of log $P_{o/w}$, there will be two (or more) different components in the mixture. For example, the log $P_{o/w}$ value of cisplatin is reported in literature as ranging from −1.7[27] to −2.5[28] and therefore spans almost 1 order of magnitude of $P_{o/w}$ ($P_{o/w} \approx 2 \times 10^{-2}$ and 3×10^{-3}, respectively). Out of this predicament, we decided to assign log $P_{o/w}$ values only for the *ligands* presented here and not for their Pt(II) complexes for a simple reason: the final pharmacophore of the complexes is identical in all cases;

DOI: 10.1021/acs.inorgchem.5b01238
Inorg. Chem. 2015, 54, 8560−8570

only variations of the (O,S) bidentate ligand contribute to changes in the complexes' polarity. It is therefore possible to attribute the complexes' relative polarity from their ligands' log $P_{o/w}$ values. For comparison, the log $P_{o/w}$ value of the respective unfunctionalized ligand **11** was determined by the same method.

Compounds **3**–**6** and **11** were subjected to the shake-flask method and the relative concentration in both phases determined by UV–visible spectrophotometry (Figure S6 for selected spectra). The log $P_{o/w}$ value was then calculated from the average absorbance in the range between 300 and 500 nm using formula 2.

$$\log\ P_{o/w} = \log\left(\frac{c_{n_{octanol}}}{c_{water}}\right) = \log\left(\frac{A^{300-500nm}_{n_{octanol}}}{A^{300-500nm}_{water}}\right) \quad (2)$$

The results are summarized in Figure 2. Compared to their silyl-protected counterparts **3**/**4**, ligands with a hydroxo group

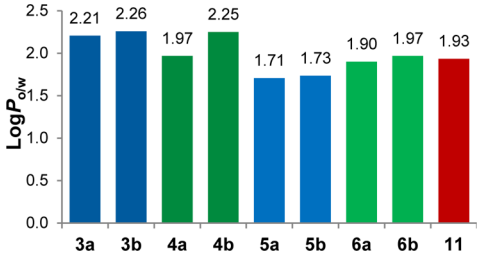

Figure 2. The log $P_{o/w}$ values of the ligands used in this study, determined by the shake-flask method using UV–vis spectrophotometry.

5/**6** give lower log $P_{o/w}$ values. Compared to the unsubstituted reference compound **11**, the effect is less pronounced. Ligand **5**, with the OH group in meta position, shows a higher degree of polarity than those with the OH group in para position (**6**); here the log $P_{o/w}$ values are almost identical to the reference compound **11**. Overall, the presence of a methyl or an ethyl group in the compound produces only minor changes in the compounds' polarity.

Antiproliferative Effects. The activity of the complexes was assessed against three model cell lines, namely, HeLa (cervix), HT29 (colon), and MCF7 (breast). Cells were exposed to the drug candidates for 72 h, and the cells' viability was quantified using the resazurin-based PrestoBlue assay. Results are comprehensively shown in Table 1. Even though all determined IC_{50} values are higher than for cisplatin, the substances showed antiproliferative activity in HeLa and MCF7 cell lines, but no activity against HT29 cell lines. Notably, meta-hydroxo complexes **9** are more active than their para-hydroxo counterparts **10** up to a degree that compounds **10** should be considered inactive also against MCF7 cells. The unsubstituted reference compound **12** is considerably more active against HT29 cells, but similar antiproliferative activity of the meta OH and unsubstituted compound was determined for HeLa and MCF7 cells. Obviously, introduction of the OH group brings forth increased selectivity toward certain cell lines with a marked difference between the two substitution patterns.

Table 1. IC_{50} Values Determined for the Investigated Compounds on Three Model Cell Lines[a]

cell line	HeLa		HT29		MCF7	
cmpd	IC_{50} [μM]		IC_{50} [μM]		IC_{50} [μM]	
9a	24.3	±5.1	>100		32.6	±0.3
9b	20.3	±3.3	>100		27.4	±3.3
10a	36.7	±0.7	>100		>100	
10b	35.3	±2.1	>100		>100	
12	21.9	±4.5	69.1	±38.6	37.3	±18.8
cisplatin	10.0	±2.1	25.0	±10.2	12.9	±3.7

[a]Results are given from three independent experiments plus standard deviation of the independently determined IC_{50} values.

Interestingly, even the ligands showed some minor antiproliferative activity, but all IC_{50} values of the ligands were determined to be >100 μM in initial experiments, so that no further biological investigation of these compounds was attempted (data not shown). The activity of the silyl-protected complexes was also tested in preliminary experiments. In these cases, solubility in culture medium was too low to reliably establish their antiproliferative activity.

Note that for compounds **9**, **10** and **12**, DMSO was needed to prepare the stock solutions. A maximum amount of 0.5 vol % DMSO was present at final concentrations close to the respective IC_{50} values. In independent experiments, it was assured that this amount of DMSO had no influence on the cellular growth level. Through microscopic inspection it was further confirmed that no precipitate was formed during the incubation period. Cisplatin, as reference, was dissolved in PBS to better represent its therapeutic application scheme.

To gain further insight into cellular response toward the drug candidates, HeLa and MCF7 cells, treated with compound **9b**, were subjected to DAPI and PI staining and examined by fluorescence microscopy. DAPI/PI counterstaining provides a useful tool to easily examine the cells' viability based on morphological features. Both dyes bind to DNA, produce fluorescence signals at specific wavelengths, and can be detected separately. DAPI is able to penetrate intact cell membranes, and it stains virtually all nuclei, including living and early apoptotic cells. PI stains nuclei only after loss of membrane integrity; therefore, it is only permanent to late apoptotic, necrotic, or dead cells.

HeLa and MCF7 cells were exposed to **9b** in concentrations below, at, and above the respective IC_{50} value for 72 h and then stained with both dyes. Fluorescence micrographs obtained are depicted in Figure 3. Both cell lines react toward drug treatment, as can be seen from the formation of condensed nuclei in DAPI-stained pictures in micrographs of cells below and at IC_{50}. Extensive drug treatment led to cellular death, as visualized by the large number of PI-stained cells at high drug concentrations.

Reactivity toward Hen Egg-White Lysozyme. *Electrospray Ionization Mass Spectrometry Results.* To characterize the reactivity of these platinum compounds with protein targets, their interaction with HEWL was analyzed through ESI MS spectrometry according to established procedures.[10] Spectral analysis allows determining the nature of the protein-bound metallic species and to define stoichiometry of the formed adducts. Representative spectra are shown in Figure 4 and in Figures S7–S11.

Incubating the samples with HEWL for 24 h proved the reactivity of the (β-hydroxy dithiocinnamic ester-O,S)Pt ((O,S)Pt) center toward this model protein. Defined adduct formation with one (O,S)Pt unit bound to the intact protein is demonstrated; two units are bound at almost neglectable intensity. No noteworthy abundance of an (O,S)Pt(DMSO)

DOI: 10.1021/acs.inorgchem.5b01238
Inorg. Chem. 2015, 54, 8560–8570

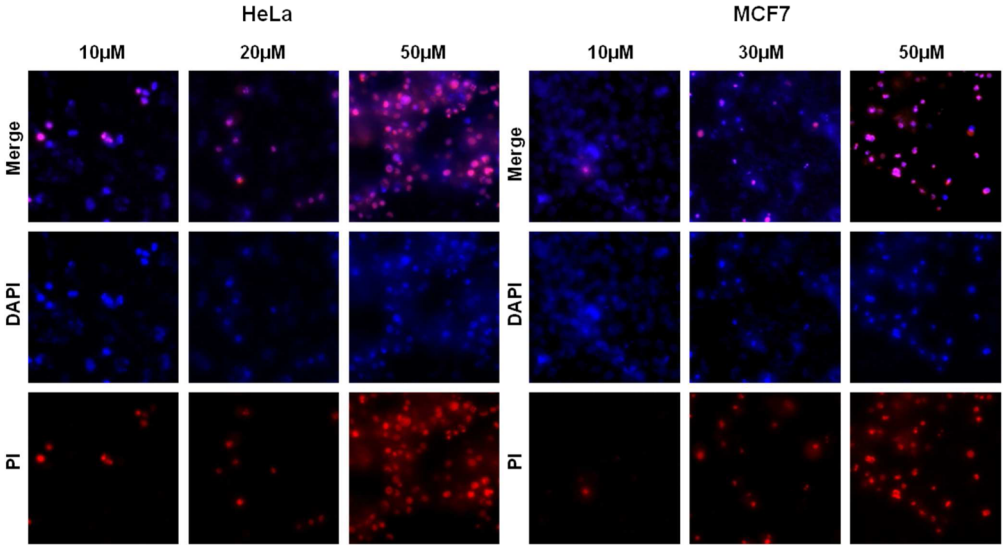

Figure 3. Fluorescence micrographs of HeLa (left) and MCF7 cells (right) exposed to **9b** in concentrations below, at, and above the determined IC_{50} value. (lower) PI staining; (middle) DAPI staining; (upper) merge. All pictures were recorded at 200-fold magnification.

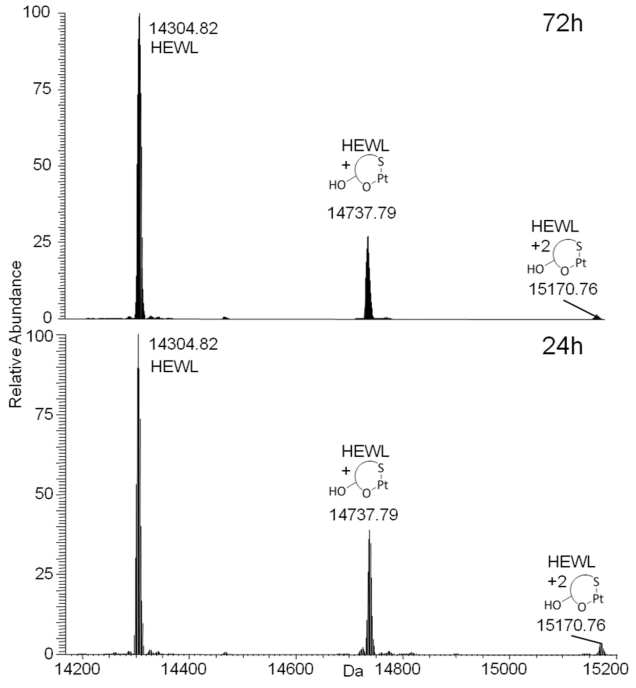

Figure 4. Deconvoluted LTQ-Orbitrap ESI mass spectra of platinum compound **9b** dissolved in 25 mM TMAA buffer, pH 7.4, after 24 h (lower) and 72 h (upper) of incubation with HEWL. Protein concentration was 100 μM with a metallodrug–protein molar ratio of 3:1.

adduct peak is observed. Elongation of the reaction time to 72 h did not alter the degree of adduct formation (Figure 4). Overall, the reactivity of the four complexes toward HEWL is comparable, with compound **9b** being the most reactive compound in this series.

A similar behavior was found for the compounds reported earlier[1] and is not surprising since only few possible binding sites are available—namely, His15, Met12, and Met105; with His15 being the highly preferred binding site for cisplatin and analogous compounds.[10,11,14]

Ultraviolet–Visible Data. In parallel, adduct formation experiments were performed using UV–visible spectrophotometry (Figure 5). The so-obtained data support the

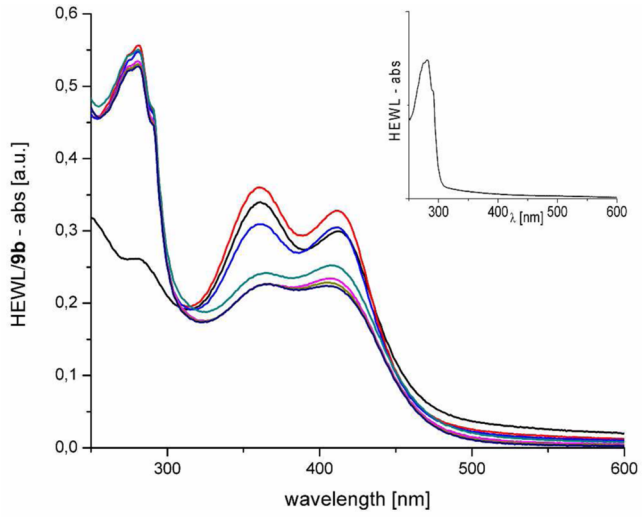

Figure 5. UV–visible time-course spectra of the reaction of compound **9b** with Lysozyme over 72 h. The Pt/HEWL ratio was 3:1; c(HEWL) = 10 μM in TMAA. Free complex (black), 0 h (red), 1 h (blue), 12 h (light green), 24 h (pink), 48 h (olive green), 72 h (gray); (inset) free HEWL in TMAA, 10 μM.

observations made by ESI MS data collection. Transformation of the complexes' initial chromophore is observed: the bands characteristic for the intact metal complex gradually lose intensity up to a static state, which is reached after ~24 h. In analogy to the UV–visible spectra of the compounds in absence of a biomolecule, these changes are attributed to gradual hydrolysis of the chloride ligand and eventually by the DMSO ligand, followed by binding of the biomolecule. The time development of these spectra seems to be in good accordance with the amount of witnessed adduct formation in the ESI data.

The chromophores of the protein and thus its overall structure, respectively their active centers, do not seem to be affected by metal binding, an observation which is also in good

DOI: 10.1021/acs.inorgchem.5b01238
Inorg. Chem. 2015, 54, 8560–8570

agreement with the ESI measurements, where intact proteins are witnessed.

X-ray Structure Determination of Hen Egg-White Lysozyme Adducts. Since ESI MS and UV−visible spectroscopic data suggest that the compounds interact with proteins, we tried to gain further insight into the molecular basis of the compounds' protein recognition by solving the structures of the adducts formed in the reaction between the two compounds **9a** or **9b**, separately, and HEWL. Single crystals of HEWL-**9a** and HEWL-**9b** adducts (Figure 6) were obtained through soaking experiments using ethylene glycol as precipitant and diffract at high resolution (1.89 and 2.15 Å for HEWL-**9a** and HEWL-**9b**, respectively).

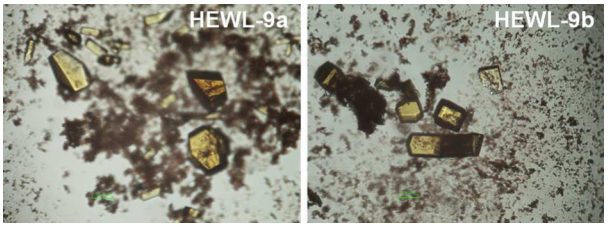

Figure 6. Crystals of HEWL-**9a** (left) and HEWL-**9b** adducts (right).

The structures of the two adducts HEWL-**9a** and HEWL-**9b** are very similar. The root-mean-square deviations of the carbon alpha (CA) atoms for the two structures are as low as 0.10 Å. Both compounds bind to the protein close to reactive His15 (Figure 7).

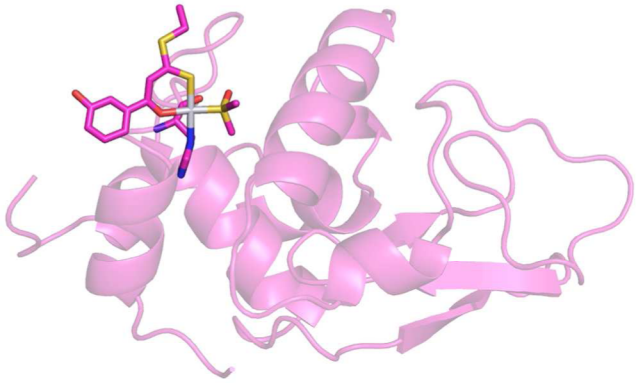

Figure 7. Cartoon representation of the HEWL-**9b** structure. The side chain of His15 and the **9b** moiety bound to the protein are also shown.

In both adducts, the chlorido ligand is lost and replaced by the ND1 atom of the side chain of His15. The electron density map is well-defined for all atoms of the complex, which retains the DMSO fragment bound to the Pt(II) center (Figure 8). The Pt-ND1 distance is in both cases ca. 2.3 Å. The (O,S)Pt(DMSO) moiety interacts with protein atoms, forming a number of stabilizing hydrophobic and hydrogen-bonding interactions. In particular, the oxygen atom of the DMSO ligand is hydrogen-bonded to the NZ atom of Lys96 and to a water molecule, whereas the methyl groups of the ligand are in contact with the CH_3 group of Thr89 and the CG1 atom of Val92.

The structures of the adducts are further stabilized by hydrogen bonds and hydrophobic interactions with atoms of the protein chains and of a symmetry-related protein molecule.

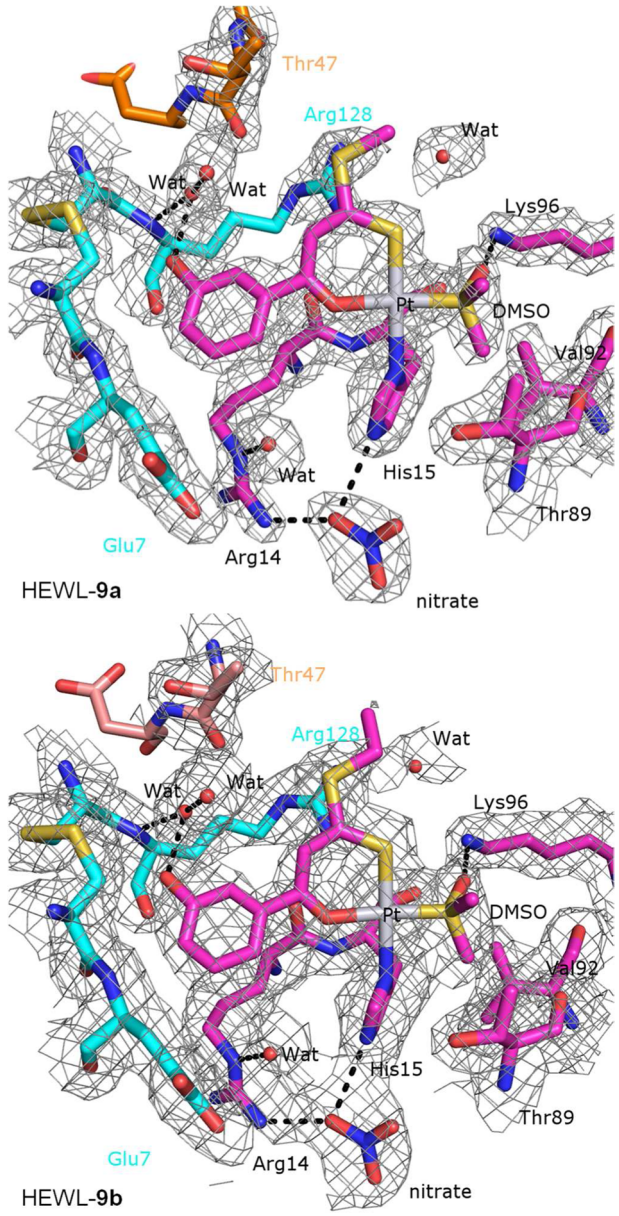

Figure 8. (upper) $2F_o - f_c$ electron density map of the **9a** binding site in the HEWL-**9a** structure (contoured at 0.8 σ, gray) obtained after model building and refinement. (lower) $2F_o - F_c$ electron density map of the **9b** binding site in the HEWL-**9b** structure (contoured at 0.6 σ, gray) obtained after model building and refinement.

In particular, the OH substituent of the phenyl group is hydrogen-bonded via a water molecule to the backbone oxygen atom of Gly126 and to the backbone N atom of Arg128.

To the best of our knowledge, these are the first structural data on the interaction between platinum(II) compounds with O,S bidentate ligands and proteins. The occupation of His15 side chains by metallodrug fragments has been observed in various structural data sets previously,[10,11,14,17,34−37] but also other amino acid side chains were found to be involved in metallodrug binding.[11,18,35,38] The retention of the DMSO ligand seems to be a distinctive feature of these particular drug candidates.

For comparison, in a recent study the formation of metallodrug-HEWL adducts was monitored by ESI MS and UV−vis in pure DMSO. Of the bis-amine metal compounds

DOI: 10.1021/acs.inorgchem.5b01238
Inorg. Chem. 2015, 54, 8560−8570

investigated, Pt(II) was found to bind the solvent in the protein adducts, whereas homologous Au(III) and Ru(II) compounds did not.[39] On the contrary, similar studies performed with cisplatin and carboplatin revealed no presence of DMSO at the platinum(II) center, even if high concentrations of DMSO were present in the incubation samples at crystallization conditions.[10,36] Furthermore, recent X-ray crystallographic studies on NAMI-A binding toward HEWL showed that the metal would replace all ligands, including the original DMSO ligand, by water molecules and subsequently bind Asp101 and Asp119 side chains instead of the frequently found His15.[40]

It can thus be concluded from the overall literature data and data obtained in this study that retention of the DMSO ligand at the metal center is not a general observation for metallodrug-HEWL adducts and also depends on the incubation conditions.

DISCUSSION

A class of novel platinum(II) compounds based on bidentate O,S-binding β-hydroxy dithiocinnamic acid esters was recently established.[1] These compounds were reported to manifest relevant antiproliferative properties in vitro and to overcome to a large extent intrinsic resistance to cisplatin. Thus, it is likely that these novel platinum compounds may act through a mechanism of action that is distinct from classical anticancer platinum drugs. Unfortunately, those compounds are characterized by a limited solubility in aqueous media that greatly hinders pharmaceutical application and further mechanistic studies.

This led us to perform a number of chemical modifications on the general scaffold, aimed toward improving aqueous solubility while conserving the favorable biological properties. In particular, a hydroxo substituent was positioned on the aromatic moiety, while the alkyl chain on the sulfur atom was kept at a minimum length of one or two carbon atoms only.

On the basis of these modifications we obtained four novel platinum(II) complexes showing an improved solubility profile in water, as shown by measurements of the water/*n*-octanol partition coefficient of the respective ligands. The main chemical features of these compounds were then characterized in comparison to those of the previously investigated reference compound **12**. On the basis of the analytical data, it can be demonstrated that the electronic structural features of the chelating unit are retained upon modification of the aromatic unit.

We further analyzed the compounds' stability in TMAA buffer, the reactivity with the model protein HEWL, and their antiproliferative actions.

Notably the four complexes **9**/**10** manifest a profile of stability in TMAA buffer quite similar to that of the reference compound **12**; spectral changes are observed with time that are ascribed to progressive hydrolysis of the chlorido ligand.

It is highlighted through ESI mass spectrometric analyses that protein derivatives are formed containing the (O,S)Pt unit in the intact protein molecule. The O,S bidentate ligand is invariantly conserved upon protein binding, whereas chloride and DMSO are lost. The reactivity of the meta-hydroxo compounds toward HEWL seems to be slightly enhanced compared to the para-substituted model complexes.

Also crystallographic evidence of protein binding is given. Molecular structures of **9a** and **9b** bound to His15 of the intact protein support our hypothesis of a distinctive binding mode of these compounds toward certain amino acid side chains. They further demonstrate that chloride represents the preferred leaving group and that the DMSO ligand *can* be retained upon protein binding. Obviously, hydrogen bonds of the (O,S) ligand and also of DMSO-O toward nearby side chains stabilize the metal unit's position within the protein. In the ESI mass spectra of HEWL adducts, no evidence of the presence of DMSO is found. It is however unlikely that this finding is merely an artifact of the ionization process, since at least some low abundance of an (O,S)Pt(DMSO) adduct should be visible in that case. Instead, the different experimental conditions might lead to a slightly altered binding mode.

All these findings point toward selective binding of the (O,S) Pt units toward distinctive amino acid side chains. This may represent a key feature of the compounds' mode of action, since in recent times, awareness of the role of proteins as crucial targets in the anticancer activity of metal compounds has grown and become a main focus of metal-based anticancer research.[4,41]

Finally the biological properties of compounds **9**/**10** and **12** were comparatively assayed in a panel of three cancer cell lines. When compared to the parent compound **12**, activity of the meta-substituted compounds **9** is similar, while reduced antiproliferative activity is observed in the case of para-substituted compounds **10**.

This marked difference in the activity based on the position of the OH group in the aromatic unit on the one hand and the insignificant differences observed upon alteration of the chain length on the other hand may be based on the slightly enhanced solubility profile of compounds **9**. It might further also imply a differentiated response of cellular mechanisms toward the respective compounds. These could involve active uptake mechanisms, as discussed for cisplatin to occur, for example, via the copper chaperone CTR1[42] or also other intracellular processes involved in drug depletion and cellular repair processes, as described in several recent reviews.[42−45]

Overall, compounds **9a** and **9b**, bearing a hydroxo group in meta position, seem to be the more promising candidates for further drug development. Their para-substituted counterparts not only possess reduced solubility in aqueous medium but also their activity toward the selected model cell lines as well as their reactivity toward model proteins seems to concur with these considerations.

ASSOCIATED CONTENT

Supporting Information

The Supporting Information is available free of charge on the ACS Publications website at DOI: 10.1021/acs.inorgchem.5b01238.

Elemental analysis, NMR, IR, and MS data of precursor materials, additional UV−vis spectral data including DFT results and time-dependent spectral profiles, ESI MS spectra of Pt-HEWL adducts, crystallographic statistical data. (PDF)

Accession Codes

Crytallographic data of HEWL-**9** adducts was furthermore deposited in the Protein Data Bank under the accession codes 4Z41 and 4Z3M.

AUTHOR INFORMATION

Corresponding Authors

*Fax: (+39) 081 674090. E-mail: antonello.merlino@unina.it. (A.M.)

DOI: 10.1021/acs.inorgchem.5b01238
Inorg. Chem. 2015, 54, 8560−8570

*Fax: (+39) 055 4573385. E-mail: luigi.messori@unifi.it. (L.M.)
*Fax: (+49) 3641 948102. E-mail: wolfgang.weigand@uni-jena.de. (W.W.)

Notes

The authors declare no competing financial interest.

■ ACKNOWLEDGMENTS

The Authors wish to thank M. Hartlieb (Jena) for contributions to the chemical synthesis of the molecules described herein as well as E. Michelucci (CISM, Florence) for assistance in recording ESI MS spectra. COST Actions CM1105 (STSM-CM1105-131014-050336) and the DAAD Vigoni Program are gratefully acknowledged for travel grants. C.M. thanks Carl-Zeiss-Stiftung as well as Studienstiftung des deutschen Volkes for scholarships. Umicore AG & Co. KG is acknowledged for a generous gift of K_2PtCl_4. This work is also supported by the Cluster of Excellence RESOLV (EXC 1069) funded by the Deutsche Forschungsgemeinschaft DFG (N. M.-L.). G.F. and A.M. thank M. Amendola and G. Sorrentino for technical assistance. Dedicated to Prof. Christian Robl (Univ. of Jena) on the occasion of his 60th birthday.

■ REFERENCES

(1) Mügge, C.; Liu, R.; Görls, H.; Gabbiani, C.; Michelucci, E.; Rüdiger, N.; Clement, J. H.; Messori, L.; Weigand, W. *Dalton Trans.* **2014**, *43*, 3072−3086.
(2) Kelland, L. *Nat. Rev. Cancer* **2007**, *7*, 573−584.
(3) Esteban-Fernández, D.; Moreno-Gordaliza, E.; Canas, B.; Palacios, M. A.; Gómez-Gómez, M. M. *Metallomics* **2010**, *2*, 19−38.
(4) Bischin, C.; Lupan, A.; Taciuc, V.; Silaghi-Dumitrescu, R. *Mini-Rev. Med. Chem.* **2011**, *11*, 214−224.
(5) Groessl, M.; Hartinger, C. G. *Anal. Bioanal. Chem.* **2013**, *405*, 1791−1808.
(6) Pinato, O.; Musetti, C.; Farrell, N. P.; Sissi, C. *J. Inorg. Biochem.* **2013**, *122*, 27−37.
(7) Moeller, C.; Tastesen, H. S.; Gammelgaard, B.; Lambert, I. H.; Sturup, S. *Metallomics* **2010**, *2*, 811−818.
(8) Arnesano, F.; Losacco, M.; Natile, G. *Eur. J. Inorg. Chem.* **2013**, *2013*, 2701−2711.
(9) Hermann, G.; Heffeter, P.; Falta, T.; Berger, W.; Hann, S.; Koellensperger, G. *Metallomics* **2013**, *5*, 636−647.
(10) Casini, A.; Mastrobuoni, G.; Temperini, C.; Gabbiani, C.; Francese, S.; Moneti, G.; Supuran, C. T.; Scozzafava, A.; Messori, L. *Chem. Commun.* **2007**, No. 2, 156−158.
(11) Messori, L.; Marzo, T.; Michelucci, E.; Russo Krauss, I.; Navarro-Ranninger, C.; Quiroga, A. G.; Merlino, A. *Inorg. Chem.* **2014**, *53*, 7806−7808.
(12) Šamalikova, M.; Grandori, R. *J. Mass Spectrom.* **2005**, *40*, 503−510.
(13) Blake, C. C. F.; Koenig, D. F.; Mair, G. A.; North, A. C. T.; Phillips, D. C.; Sarma, V. R. *Nature* **1965**, *206*, 757−761.
(14) Tanley, S. W. M.; Diederichs, K.; Kroon-Batenburg, L. M. J.; Levy, C.; Schreurs, A. M. M.; Helliwell, J. R. *Acta Crystallogr., Sect. F: Struct. Biol. Commun.* **2014**, *70*, 1135−1142.
(15) Schubert, K.; Saumweber, R.; Görls, H.; Weigand, W. *Z. Anorg. Allg. Chem.* **2003**, *629*, 2091−2096.
(16) Schubert, K.; Alpermann, T.; Niksch, T.; Görls, H.; Weigand, W. *Z. Anorg. Allg. Chem.* **2006**, *632*, 1033−1042.
(17) Messori, L.; Scaletti, F.; Massai, L.; Cinellu, M. A.; Gabbiani, C.; Vergara, A.; Merlino, A. *Chem. Commun.* **2013**, *49*, 10100−10102.
(18) Messori, L.; Cinellu, M. A.; Merlino, A. *ACS Med. Chem. Lett.* **2014**, *5*, 1110−1113.
(19) Russo Krauss, I.; Messori, L.; Cinellu, M. A.; Marasco, D.; Sirignano, R.; Merlino, A. *Dalton Trans.* **2014**, *43*, 17483−17488.
(20) Otwinowski, Z.; Minor, W. In *Macromolecular Crystallography, Part A;* Carter, C. W., Jr., Sweet, R. M., Eds.; Methods in Enzymology; Academic Press: New York, 1997; Vol. *276*, pp 307−326.
(21) Vergara, A.; Russo Krauss, I.; Montesarchio, D.; Paduano, L.; Merlino, A. *Inorg. Chem.* **2013**, *52*, 10714−10716.
(22) Murshudov, G. N.; Skubák, P.; Lebedev, A. A.; Pannu, N. S.; Steiner, R. A.; Nicholls, R. A.; Winn, M. D.; Long, F.; Vagin, A. A. *Acta Crystallogr., Sect. D: Biol. Crystallogr.* **2011**, *67*, 355−367.
(23) Winn, M. D.; Ballard, C. C.; Cowtan, K. D.; Dodson, E. J.; Emsley, P.; Evans, P. R.; Keegan, R. M.; Krissinel, E. B.; Leslie, A. G. W.; McCoy, A.; McNicholas, S. J.; Murshudov, G. N.; Pannu, N. S.; Potterton, E. A.; Powell, H. R.; Read, R. J.; Vagin, A.; Wilson, K. S. *Acta Crystallogr., Sect. D: Biol. Crystallogr.* **2011**, *67*, 235−242.
(24) Emsley, P.; Lohkamp, B.; Scott, W. G.; Cowtan, K. *Acta Crystallogr., Sect. D: Biol. Crystallogr.* **2010**, *66*, 486−501.
(25) Berthod, A.; Carda-Broch, S. *J. Chromatogr. A* **2004**, *1037*, 3−14.
(26) *Off. J. Eur. Communities: Legis.* **1992**, *L383 A*, 63−73.
(27) Tetko, I. V.; Jaroszewicz, I.; Platts, J. A.; Kuduk-Jaworska, J. *J. Inorg. Biochem.* **2008**, *102*, 1424−1437.
(28) Screnci, D.; McKeage, M. J.; Galettis, P.; Hambley, T. W.; Palmer, B. D.; Baguley, B. C. *Br. J. Cancer* **2000**, *82*, 966−972.
(29) Baker, M. V.; Barnard, P. J.; Berners-Price, S. J.; Brayshaw, S. K.; Hickey, J. L.; Skelton, B. W.; White, A. H. *Dalton Trans.* **2006**, 3708−3715.
(30) Kunz, P. C.; Huber, W.; Rojas, A.; Schatzschneider, U.; Spingler, B. *Eur. J. Inorg. Chem.* **2009**, *2009*, 5358−5366.
(31) Minick, D. J.; Frenz, J. H.; Patrick, M. A.; Brent, D. A. *J. Med. Chem.* **1988**, *31*, 1923−1933.
(32) Platts, J. A.; Oldfield, S. P.; Reif, M. M.; Palmucci, A.; Gabano, E.; Osella, D. *J. Inorg. Biochem.* **2006**, *100*, 1199−1207.
(33) Maschke, M.; Lieb, M.; Metzler-Nolte, N. *Eur. J. Inorg. Chem.* **2012**, *2012*, 5953−5959.
(34) Messori, L.; Marzo, T.; Gabbiani, C.; Valdes, A. A.; Quiroga, A. G.; Merlino, A. *Inorg. Chem.* **2013**, *52*, 13827−13829.
(35) Marasco, D.; Messori, L.; Marzo, T.; Merlino, A. *Dalton Trans.* **2015**, *44*, 10392−10398.
(36) Tanley, S. W. M.; Schreurs, A. M. M.; Kroon-Batenburg, L. M. J.; Meredith, J.; Prendergast, R.; Walsh, D.; Bryant, P.; Levy, C.; Helliwell, J. R. *Acta Crystallogr., Sect. D: Biol. Crystallogr.* **2012**, *68*, 601−612.
(37) Helliwell, J. R.; Tanley, S. W. M. *Acta Crystallogr., Sect. D: Biol. Crystallogr.* **2013**, *69*, 121−125.
(38) Messori, L.; Marzo, T.; Merlino, A. *Chem. Commun.* **2014**, *50*, 8360−8362.
(39) Marzo, T.; Savić, A.; Massai, L.; Michelucci, E.; Sabo, T. J.; Grguric-Šipka, S.; Messori, L. *BioMetals* **2015**, *28*, 425−430.
(40) Messori, L.; Merlino, A. *Dalton Trans.* **2014**, *43*, 6128−6131.
(41) Casini, A.; Reedijk, J. *Chem. Sci.* **2012**, *3*, 3135−3144.
(42) Arnesano, F.; Natile, G. *Coord. Chem. Rev.* **2009**, *253*, 2070−2081.
(43) Wang, D.; Lippard, S. J. *Nat. Rev. Drug Discovery* **2005**, *4*, 307−320.
(44) Rabik, C. A.; Dolan, M. E. *Cancer Treat. Rev.* **2007**, *33*, 9−23.
(45) Dasari, S.; Bernard Tchounwou, P. *Eur. J. Pharmacol.* **2014**, *740*, 364−378.

DOI: 10.1021/acs.inorgchem.5b01238
Inorg. Chem. 2015, 54, 8560−8570